ORAL DISEASES

Oral Diseases (2010) 16, 624–630. doi:10.1111/j.1601-0825.2009.01643.x

www.wiley.com

ORIGINAL ARTICLE

In vitro behavior of MC3T3-E1 preosteoblast with different annealing temperature titania nanotubes

WQ Yu, YL Zhang, XQ Jiang, FQ Zhang

Department of Prosthodontics, Ninth People's Hospital, Shanghai Jiao Tong University School of Medicine, Shanghai Key Laboratory of Stomatology, Shanghai, China

OBJECTIVE: Titanium oxide nanotube layers by anodization have excellent potential for dental implants because of good bone cell promotion. It is necessary to evaluate osteoblast behavior on different annealing temperature titania nanotubes for actual implant designs.

MATERIALS AND METHODS: Scanning Electron Microscopy, X-Ray polycrystalline Diffractometer (XRD), X-ray photoelectron Spectroscope, and Atomic Force Microscopy (AFM) were used to characterize the different annealing temperature titania nanotubes. Confocal laser scanning microscopy, MTT, and Alizarin Red-S staining were used to evaluate the MC3T3-E1 preosteoblast behavior on different annealing temperature nanotubes.

RESULTS: The tubular morphology was constant when annealed at 450°C and 550°C, but collapsed when annealed at 650°C. XRD exhibited the crystal form of nanotubes after formation (amorphous), after annealing at 450°C (anatase), and after annealing at 550°C (anatase/rutile). Annealing led to the complete loss of fluorine on nanotubes at 550°C. Average surface roughness of different annealing temperature nanotubes showed no difference by AFM analysis. The proliferation and mineralization of preostoblasts cultured on anatase or anatase/rutile nanotube layers were shown to be significantly higher than smooth, amorphous nanotube layers.

CONCLUSION: Annealing can change the crystal form and composition of nanotubes. The nanotubes after annealing can promote osteoblast proliferation and mineralization *in vitro*.

Oral Diseases (2010) **16**, 624–630

Keywords: nanotube layer; annealing; preosteoblast; proliferation; mineralization

Correspondence: Fu-qiang Zhang, Department of Prosthodontics, School of Stomatology, Ninth People's Hospital, School of Medicine, Shanghai JiaoTong University, Shanghai, China. Tel: +86 21 23271699 (ext. 5694), Fax: +86 21 63136856, E-mail: fredzc@online.sh.cn

Received 31 July 2009; revised 12 October 2009; accepted 14 October 2009

Introduction

Titanium (Ti) and its alloys such as Ti-6Al-4V and Ti-6Al-7Nb are widely used as implantation materials because of their good mechanical properties, excellent corrosion resistance, and biocompatibility (Linder *et al*, 1988; Albrektsson and Sennerby, 1990). Although pure Ti metal has a natural, thin TiO_2 passive layer, it is susceptible to the formation of fibrous tissue because of smooth and dense TiO_2, which leads to implant mobility and subsequent failure (Le Guéhennec *et al*, 2007). So, titanium-based implants must be able to recruit bone formation effectively.

Osseointegration was the hallmark of success in endosseous implants in the 1980s (Roberts, 1988). Chemical composition and topography of implant surface play an important role in affecting the rate and extent of osseointegration (Albrektsson *et al*, 1981; Boyan *et al*, 1993). To further control the osseointegration of titanium-based implants, many surface modification methods have been applied, such as titania or hydroxyapatite coating by plasma spraying and various types of topography coating by acid-etching or anodization on implant surfaces (Le Guéhennec *et al*, 2007).

As the natural environment to which osteoblast is accustomed to is in the nanometer regime, the researchers began to simulate the topography of normal bone on implant surfaces (Mendon *et al*, 2008). Many chemical compositions have been developed to create nanorough surface of implants. For example, Webster *et al* (1999, 2000) reported that the osteoblast adhesion and function on nanophase alumina and titania were significantly greater than conventional ceramics. At the same time, Webster and Ejiofor (2004) reported that osteoblast adhesion on nanophase metals was significantly greater than conventional metals. Various types of nano-sized topographies have been prepared to enrich the implant materials coating, for example, osteoblast responses were evaluated by studying their adhesion and function cultured on the nanoporous alumina membranes (Popat *et al*, 2005; Swan *et al*, 2005). In addition, Elias *et al* (2002) found that osteoblast cultured on nanometer

diameter carbon fibers synthesized more alkaline phosphatase and deposited more calcium compared with larger-diameter carbon fibers. Recently, the modification of implant surface roughness at the nanoscale level becomes one of the major research interest (Gustavo *et al*, 2008).

Recently, TiO_2 nanotube layers by anodization have received considerable attention in implant materials (Oh *et al*, 2006; Popat *et al*, 2007; Das *et al*, 2009; Yao *et al*, 2008). Growth of Hydroxyapatite showed a significantly accelerated kinetics on anodic TiO_2 nanotubes or chemically treated titanium oxide nanotubes (Oh *et al*, 2005; Tsuchiya *et al*, 2006). The adhesion and function of osteoblast (bone-forming cell) cultured on TiO_2 nanotube layer by anodization could be increased compared with their unanodized counterparts (Oh *et al*, 2006; Popat *et al*, 2007; Das *et al*, 2009; Yao *et al*, 2008). Von Wilmowsky *et al* (2009) studied peri-implant bone formation of TiO_2 nanotube layer *in vivo*. Their results showed that the TiO_2 nanotube layer could influence bone formation and bone development. Recently, few reports have demonstrated that the diameter of nanotube layers could significantly influence the adhesion and differentiation of osteoblast (bone-forming cell) (Brammer *et al*, 2009; Oh *et al*, 2009). In these studies, most of the nanotube layers were unannealed (Yao *et al*, 2008; Von Wilmowsky *et al*, 2009) or annealed at one temperature, such as 500°C (Oh *et al*, 2006, 2009; Brammer *et al*, 2008, 2009). It has been proved that the chemical composition and crystal form changed greatly after annealing at different temperatures (Macak *et al*, 2007). As the chemical composition and crystal form of implants surface may affect their biological and clinical behavior (Le Guéhennec *et al*, 2007), the purpose of this work is to study whether the behavior of MC3T3-E1 preosteoblast would be affected when cultured on different annealing temperature titania nanotubes. The characterizations of nanotube layers were analyzed by Scanning Electron Microscopy (SEM), X-ray diffraction (XRD), X-ray Photoelectron Spectroscope (XPS), and Atomic Force Microscopy (AFM). The behavior of preosteoblast was evaluated by morphology, proliferation, and mineralization.

Materials and methods

TiO_2 nanotube layer preparation

Titanium thin foils (0.25 mm thick) with a purity of 99.5% (Alfa Aesar, Tianjin, China) were used to prepare the samples. Prior to anodization, titanium substrates were immersed in a mixture of [2 ml 48% HF, 3 ml 70% HNO_3 (both reagent grade chemicals) and 100 ml deionized water] for 5 min to remove the naturally formed oxide layer, then rinsed in deionized water, and dried in nitrogen stream. Titanium oxide nanotubes were fabricated by anodization with a potentiostat in 0.5 wt % HF solution at 20 V for 1 h (Popat *et al*, 2007). Platinum was used as the counter electrode. After anodization, the samples were rinsed with deionized water and dried in a nitrogen stream. To acquire different crystalline phase nanotube layers, the nanotubes were then annealed at 450°C, 550°C, and 650°C for 3 h in air. All the experimental specimens (1×1 cm^2) used for cell growth were sterilized in an autoclave at 120°C for 30 min. The Ti foil was polished by SiC emery paper (No. 1200 grit size) for use as a control group sample.

Characterization

X-Ray Polycrystalline Diffractometer (XRD) graphs were obtained using a XRD (Bruker-Axs, Karlsruhe, Germany) with a copper Kα radiation at 40 kV and 100 mA. Scanning was recorded on a KEVEX detector between 20° (2θ) and 80° (2θ) with a 10°min^{-1} scan speed. The results of XRD spectra were compared with titanium (JCPDS No. 44-1294) and TiO_2 (anatase and rutile; JCPDS No. 21-1272 and JCPDS No. 21-1276) standards.

The microstructures of different temperature annealed nanotube layers were observed by SEM (FEI SIRION 200, Hillsboro, USA). The cross-section photograph was obtained by observing mechanically fractured samples. All samples were sputter-coated with Au before imaging using a HUMMER I Sputtercoater for 3 min.

The composition of different temperature annealed nanotube layers was examined by XPS (VG Scientific Microlab 310F, East Grinstead, UK). The analysis was performed utilizing a monochromatic Al Kα electrode at 15 kV and 150 W at a 45° take-off angle. The sampling depth was measured about 3 nm. The Service Physics ESCAVB Graphics Viewer (Bristol, UK) program was used to determine peak areas.

Average surface roughness of the samples was analyzed by an Atomic Force Microscope (Bioscope Veeco, Santa Barbara, CA, USA) to compare different annealing temperature titania nanotubes. Commercially available tip curvature radius used in this study was <10 nm. The measurements were conducted under tapping mode with a scan rate of 0.5 HZ. The scan area was 1×1 μm^2. The average surface roughness was estimated with the aid of Nanoscope imaging software. Measurements were run in triplicate per sample.

Preosteoblast culture

MC3T3-E1 mouse preosteoblasts (maintained in the current research lab) were cultured in alpha-mininum essential medium (α-MEM) with 10% fetal bovine serum and 1% penicillin/streptomycin (PS) under 37°C, 5% CO_2 environment. Cells were seeded onto the experimental substrates, which were then placed on a 24-well polystyrene plate. The concentration of the cells initially seeded onto the specimen substrate was 2×10^4 cells per well. Cell mineralization was researched in osteogenic media [regular media described above plus 10 mM β-glycerol phosphate and 50 μg ml^{-1} ascorbic acid (Sigma, Shanghai, China)]. Culture media were changed every 2 or 3 days.

Morphology of adherent preosteoblast

Cells were seeded on samples for 24 h and rinsed with PBS for three times. The cells were fixed by 4% paraformaldehyde for 30 min and then rinsed with PBS. The samples were treated with 1% Triton X-100 in

PBS to permeabilize the cells for 5 min and then gently rinsed with PBS. The samples were blocked with 1% BSA for 20 min, and the action cytoskeletons were labeled by incubating with Phalloidia-TRITC (20 μg ml^{-1}, Sigma) for 30 min. After rinsing with PBS, the cell nuclei were contrast-labeled in blue by DAPI (Sigma). The samples were rinsed with PBS and then mounted on glass slides using Fluoromount (Sigma). The action cytoskeletons of cells were visualized with a confocal laser scanning microscopy (CLSM, TLS SP2, Leica, Wetzlar, Germany).

MTT proliferation assay

The cell proliferation was investigated after seeding the cells for 24 h, 48 h, and 72 h using a MTT assay. After the selected incubation periods, the samples were washed by PBS and transferred to a new 24-well polystyrene culture plate. In all, 20 μl of MTT (5 mg ml^{-1}, Sigma) and 200 μl culture medium were added to each well. After 4 h of incubation in 5% CO_2 incubator, the culture medium was removed, 200 μl of DMSO was added to each well, and the polystyrene plate was shaken for 10 min. The solutions were transferred (200 μl) to a 96-well polystyrene plate. The absorbance of each solution was measured at the wavelength of 490 nm by spectrophotometer (Safire^2 TECAN, Seestrasse, Switzerland).

Mineralization

Mineralization was investigated after seeding the cells for 2 weeks and 3 weeks using Alizarin Red-S (ARS) staining (Gregory *et al*, 2004). After the selected incubation periods, the samples were washed by PBS and transferred to a new 24-well polystyrene culture plate. The samples were fixed in ice cold 70% ethanol for 1 h, then washed three times with dH_2O, and stained with ARS (40 mM) for 20 min at room temperature. After several washes with dH_2O, the stain was desorbed with 200 μl 10% cetylpyridinium chloride (sigma) for 1 h. The dye was collected, and absorbance was read at 590 nm in spectrophotometer (Safire^2 TECAN).

Statistical analysis

The MTT and mineralization data were compared and analyzed among the groups using standard analysis of variance (ANOVA) by SPSS 11.5 software (Chicago, USA); $P < 0.05$ was considered statistically significant.

Results

Materials characterization

The crystal patterns of nanotube layers annealed at different temperatures were acquired by XRD (Figure 1). The unannealing nanotube layers had an amorphous structure (Figure 1a). After annealing at 450°C for 3 h, the amorphous nanotubes converted to anatase structure (Figure 1b). The nanotubes had a mixture of anatase and rutile structure after annealing at 550°C and 650°C for 3 h (Figure 1c,d).

The microstructures of nanotube layers annealed at different temperatures were assessed by SEM (Figure 2).

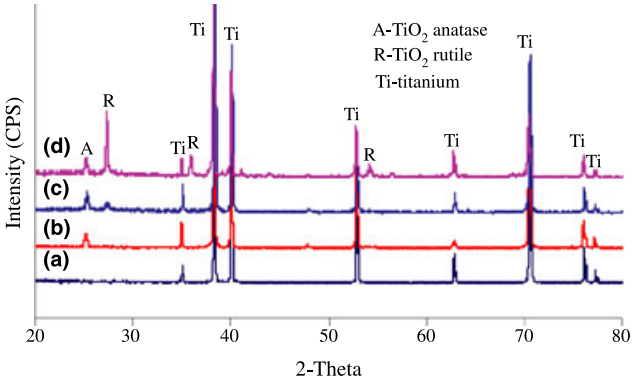

Figure 1 XRD patterns of nanotube layers **(a)** unannealed **(b)** annealed at 450°C for 3 h, **(c)** annealed at 550°C for 3 h, and **(d)** annealed at 650°C for 3 h

The diameter of nanotube layers unannealed was approximately 80 nm (Figure 2a). The cross-sections obtained from mechanically cracked samples showed the thickness that was about 400 nm (Figure 2b). After annealing at 450°C and 550°C for 3 h, the diameters (Figure 2c,d) of nanotube layers were the same as that of unannealed nanotube layer (Figure 2a). After annealing at 650°C for 3 h, a substantial collapse of the tubular morphology was seen by SEM (Figure 2e) and an exfoliation of nanotube layer is showed in (Figure 2f).

X-ray Photoelectron Spectroscope results show that the outermost layers of nanotubes unannealed and annealed at 450°C for 3 h mainly contain Ti, O, N, C, and F, but the outermost layers of smooth and nanotube layers annealed at 550°C for 3 h mainly contain Ti, O, N, and C (Table 1).

The average surface roughness of nanotubes was slightly higher than that of smooth-Ti, but the average surface roughness between different annealing temperature nanotubes showed no difference by AFM analysis (Table 2).

Morphology of adherent preosteoblast

MC3T3-E1 cell morphology on different annealing temperatures titania nanotubes was investigated using a phalloidin staining method to evaluate the actin cytoskeleton (Figure 3). The cells cultured on smooth layers exhibited a spindle-like elongated form (Figure 3a). The cells cultured on nanotube layers seem to exhibit polygonal morphology (Figure 3b–d) and spread more filopodias than smooth layers (Figure 3). Actin cytoskeleton of preosteoblast cultured on the nanotubes annealed at 450°C and 550°C (Figure 3c,d) seemed to show more regular arrangement than the smooth and the nanotubes unannealed layers(Figure 3a,b).

Cell viability and proliferation

The viability and proliferation of MC3T3-E1 preosteoblast cultured on different annealing temperatures titania nanotubes were indicated by MTT array (Figure 4). Data were analyzed by the SPSS 11.5 and the trend of cell proliferation on nanotubes at various annealing temperatures was as follows: nanotubes annealed at

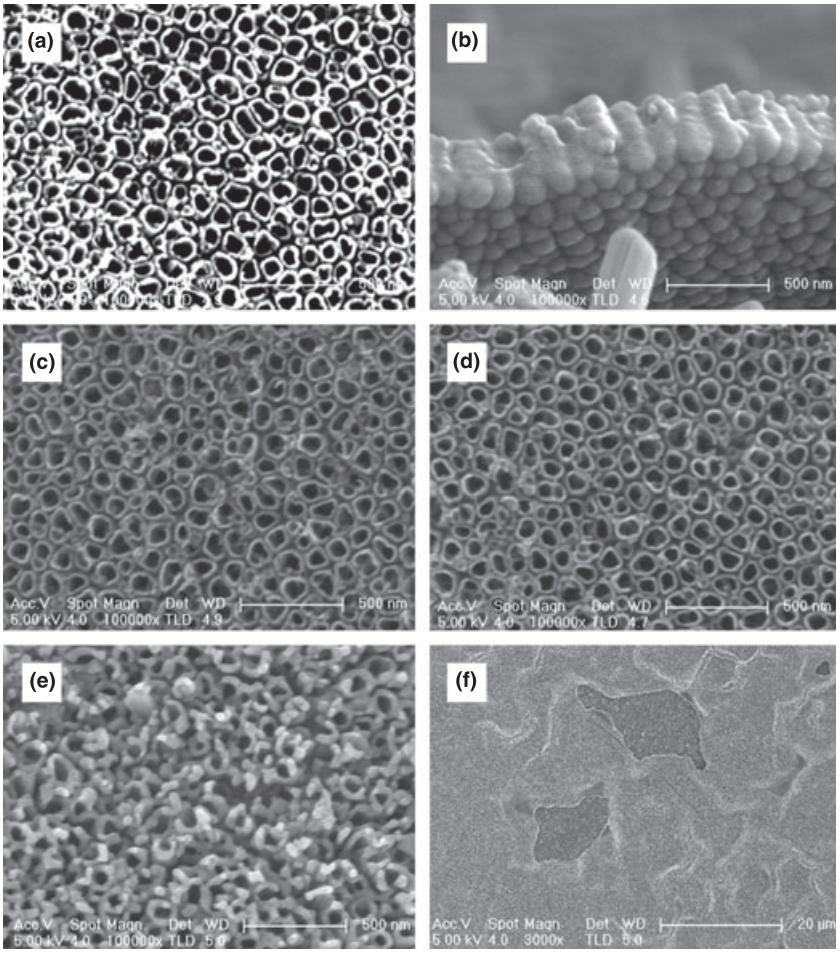

Figure 2 SEM images of nanotube layers **(a)** unannealed, **(b)** unannealed for cross-section, **(c)** annealed at 450°C for 3 h, **(d)** annealed at 550°C for 3 h, **(e)** and **(f)** annealed 650°C for 3 h

550°C > nanotubes annealed at 450°C > unannealed nanotubes > smooth ($P < 0.05$) after 72 h of culture.

Mineralization

MC3T3-E1 preosteoblast was cultured on different annealing temperatures titania nanotubes in osteogenic medium. Mineralization was investigated using Alizarin Red-S (ARS) staining. As shown in Figure 5, the trend of cell mineralization on nanotubes annealing at various temperature was as follows: nanotubes annealed at 550°C > nanotubes annealed at 450°C > unannealed nanotubes > smooth ($P < 0.05$) after 3 weeks of culture.

Discussion

Morphology of adherent osteoblast plays an important role in regulating cell behaviors (Qu *et al*, 1996). In our studies, the results showed that the cells cultured on nanotube layers spread better and extended more filopodias than smooth layers. The reason is that the nanotubes not only exhibited larger surface areas and higher surface roughness, but also provided an interlocked cell configuration (Oh *et al*, 2006). Recently, Brammer *et al* (2008) reported that the nanotube layers could enhance the endothelial cell mobility and increases cell to cell interactions because of the nanoscale cues. In our results, spreading more filopodias on nanotubes seemed to exhibit the trend. Cytoskeleton is thought to have a significant role in cell growth and differentiation (Qu *et al*, 1996). Recently, some reports showed that

Table 1 Atomic percentage of selective elements in outermost layers of nanotube layers at different annealing temperatures by X-ray Photoelectron Spectroscopy

Group	*Ti*	*O*	*N*	*C*	*F*
Smooth-Ti	14.680	61.809	3.643	19.868	0
Nanotubes unannealed	16.902	47.011	1.94	31.14	3.008
Nanotubes annealed at 450°C	20.096	53.815	1.705	23.675	0.726
Nanotubes annealed at 550°C	17.986	51.238	2.796	27.796	0

Table 2 Average surface roughness of different annealing temperature titania nanotubes by AFM analysis

Group	*Average surface roughness (nm)*
Smooth-Ti	6.18 ± 0.49
Nanotubes unannealed	13.34 ± 2.22*
Nanotubes annealed at 450°C	10.25 ± 0.38*
Nanotubes annealed at 550°C	10.66 ± 1.92*

Values are mean ± s.d.; $n = 3$; *$P < 0.05$ compared with smooth-Ti.

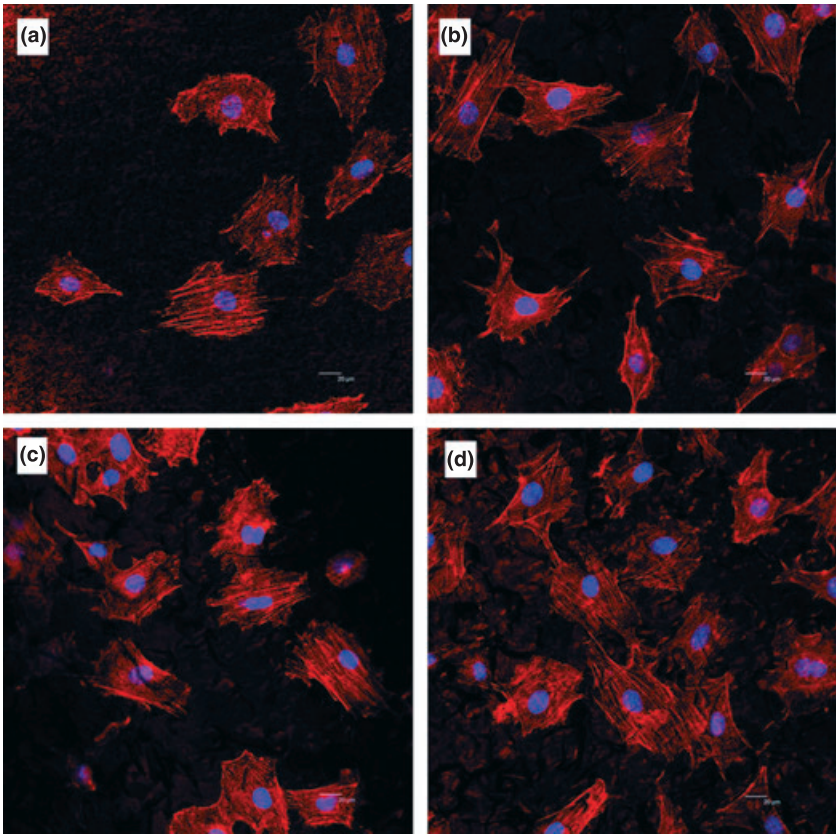

Figure 3 Phalloidin staining of the actin cytoskeleton of adherent MC3T3-E1 osteoblast after 24 h of incubation on the different samples: smooth **(a)**, unannealed nanotube layers **(b)**, annealed nanotube layers at 450°C **(c)** and 550°C **(d)**

the cytoskeleton of osteoblast cultured on anatase could exhibit regular arrangement, which influenced the cell proliferation and osteogenic gene expression (He *et al*, 2008; Yang *et al*, 2009). In our studies, the actin cytoskeleton of preosteoblast cultured on the nanotubes with anatase or anatase/rutile seemed to show more regular arrangement than the smooth and the nanotubes with amorphous structure. The results of proliferation and mineralization indicated that the regular cytoskeleton of cells influenced the preosteoblast behaviors.

Chemistry of substratum is an important factor influencing the osteoblast responses (Le Guéhennec *et al*, 2007). In our studies, the chemistry of different nanotube layers was studied by XPS. The results showed that the substratums had similar Ti, O, C, and N content, but F content was significantly different between different nanotube layers. In the literature, a small quantity F of implant surfaces can support greater proliferation and differentiation (Cooper *et al*, 2006; Guo *et al*, 2007). For exmple, Cooper *et al* (2006) reported that fluoride ion modification of the TiO_2 grit-blasted surface not only increased osteoblastic proliferation and differentiation *in vitro,* but also enhanced interfacial bone formation *in vivo*. Furthermore, the results by Guo *et al* (2007) showed that additional HF treatment of the TiO_2 grit-blasted surface enhanced the adherent cell osteo-inductive and bone specific mRNA expression. In these studies, a little F was observed on nanotube layers unannealed and annealed at 450°C, but the proliferation and mineralization of adherent

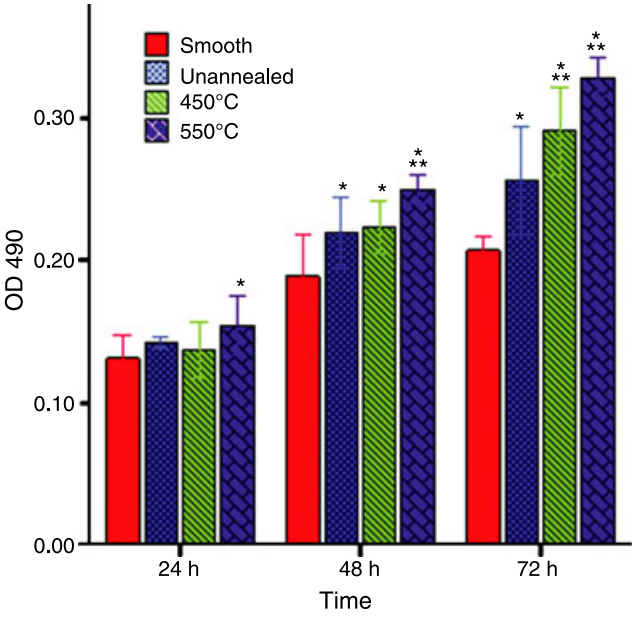

Figure 4 MTT assay data showing the viability and proliferation of osteoblast cultured on smooth, unannealed nanotube layers, annealed nanotube layers at 450°C and 550°C after 24 h, 48 h, and 72 h of incubation. The error bars in the figure represent the standard deviation for three samples for each data. $*P < 0.05$ compared with smooth and $**P < 0.05$ compared with unannealed nanotubes

preosteoblast on them showed lower than that on anatase/rutile phase nanotube layers, which had no F element. Therefore, the crystal structure of nanotube

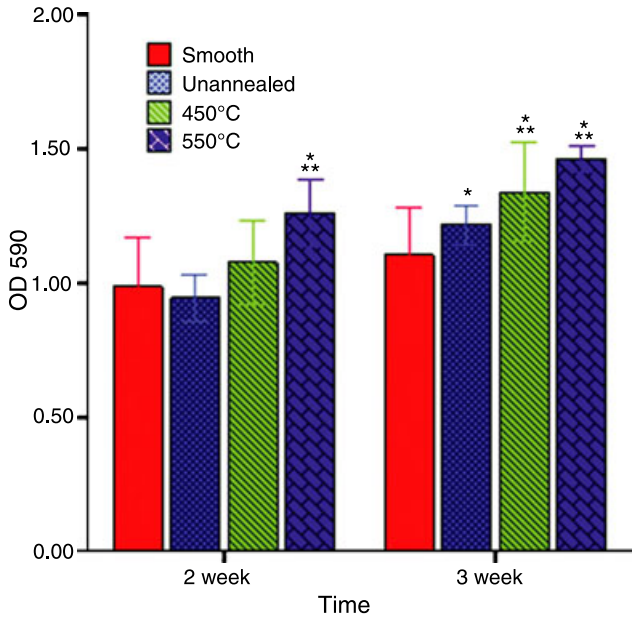

Figure 5 The mineralization of MC3T3-E1 preosteoblast cultured on different annealing temperatures titania nanotubes after 2 weeks and 3 weeks. The error bars in the figure represent the standard deviation for three samples for each data. $*P < 0.05$ compared with smooth and $**P < 0.05$ compared with unannealed nanotubes

layers can over-ride the chemistry effect and plays a main role in cell proliferation and mineralization.

In the literature, many results indicate that apatite can be formed more easily on anatase than on rutile or amorphous (Li *et al*, 2004), and growth of osteoblast cultured on anatase coating can be significantly increased compared with other phase coating (He *et al*, 2008; Palmieri *et al*, 2008; Sollazzo *et al*, 2008). For example, He *et al* (2008) reported that the adhesion and proliferation of osteoblast cultured on anatase phase nanotopography titania showed significantly enhanced compared with rutile and amorphous films. In our studies, the anatase or anatase/rutile nanotube layers showed accelerated growth and mineralization of osteoblast than amorphous nanotube layers. Upregulated genes expression could partly explain the better activity of cell cultured on anatase and anatase/rutile nanotube layers. More recently, by using DNA microarrays containing 20 000 genes, Sollazzo *et al* (2008) found that the anatase coating can increase transcription of some mRNAs, which enhance osteoblast activity. Similar result was reported by Palmieri *et al* (2008) on anatase nanosurface, but more experiments would be needed to verify this phenomenon.

Conclusion

In this study, we demonstrated that the nanotube layers were convenient for cell spreading compared with smooth layers. The proliferation and mineralization of preosteoblast cultured on anatase or anatase/rutile nanotube layers showed significantly higher than smooth layer and amorphous nanotube layers, which means the crystal structure of nanotube layers can override the chemistry effect and plays a main role in cell proliferation and mineralization. Thus, further studies are directed towards an osseointegration assessment of different crystal nanotube layers *in vivo*.

Acknowledgements

The authors would like to thank Bang-shang Zhu (Instrumental Analysis Center, Shanghai Jiao Tong University) and Xiu-li Zhang (Oral Bioengineering Lab, Ninth People's Hospital, School of Medicine, Shanghai Jiao Tong University) for helpful assistance in experiments. This work was Supported by Shanghai Leading Academic Discipline Project (Project Number: S30206), Science and Technology committee of Shanghai (08DZ2271100 and 0852nm02900), and Shanghai Leadind Academic Discipline Project (T0202).

References

Albrektsson T, Sennerby L (1990). Direct bone anchorage of oral implants: clinical and experimental considerations of the concept of osseointegration. *Int J Prosthodont* **3:** 30–41.

Albrektsson T, Branemark PI, Hansson HA *et al* (1981). Osseointegrated titanium implants. Requirements for ensuring a long-lasting, direct bone-to-implant anchorage in man. *Acta Orthop Scand* **52:** 155–170.

Boyan BD, Schwartz Z, Hambleton JC (1993). Response of bone and cartilage cells to biomaterials in vivo and in vitro. *J Oral Implantol* **19:** 116–122.

Brammer KS, Oh S, Gallagher JO *et al* (2008). Enhanced cellular mobility guided by TiO_2 nanotube surfaces. *Nano Lett* **8:** 786–793.

Brammer KS, Oh S, Cobb CJ *et al* (2009). Improved bone-forming functionality on diameter-controlled TiO(2) nanotube surface. *Acta Biomater* **5:** 3215–3223 [Epub ahead of print].

Cooper LF, Zhou Y, Takebe J *et al* (2006). Fluoride modification effects on osteoblast behavior and bone formation at TiO_2 grit-blasted c.p. titanium endosseous implants. *Biomaterials* **27:** 926–936.

Das K, Bose S, Bandyopadhyay A (2009). TiO(2) nanotubes on Ti: influence of nanoscale morphology on bone cell-materials interaction. *J Biomed Mater Res A* **90:** 225–237.

Elias KL, Price RL, Webster TJ (2002). Enhanced functions of osteoblasts on nanometer diameter carbon fibers. *Biomaterials* **23**(15)**:** 3279–3287.

Gregory CA, Gunn WG, Peister A *et al* (2004). An Alizarin red-based assay of mineralization by adherent cells in culture:Comparison with cetylpyridinium chloride extraction. *Anal Biochem* **329:** 77–84.

Guo J, Padilla RJ, Ambrose W *et al* (2007). The effect of hydrofluoric acid treatment of TiO_2 grit blasted titanium implants on adherent osteoblast gene expression in vitro and in vivo. *Biomaterials* **28:** 5418–5425.

He J, Zhou W, Zhou X *et al* (2008). The anatase phase of nanotopography titania plays an important role on osteoblast cell morphology and proliferation. *J Mater Sci Mater Med* **19:** 3465–3472.

Le Guéhennec L, Soueidan A, Layrolle P *et al* (2007). Surface treatments of titanium dental implants for rapid osseointegration. *Dent Mater* **23:** 844–854.

Li LH, Kong YM, Kim HW *et al* (2004). Improved biological performance of Ti implants due to surface modification by micro-arc oxidation. *Biomaterials* **25:** 2867–2875.

Linder L, Carlsson A, Marsal L *et al* (1988). Clinical aspects of osseointegration in joint replacement. *J Bone Joint Surg [Br]* **70:** 550–555.

Macak JM, Tsuchiya H, Ghicov A *et al* (2007). TiO_2 nanotubes: self-organized electrochemical formation, properties and applications. *Curr Opin Solid State Mater Sci* **11:** 3–18.

Mendon G, Mendon DBS, Francisco JL *et al* (2008). Advancing dental implant surface technology-From micronto nanotopography. *Biomaterials* **29:** 3822–3835.

Oh SH, Finõnes RR, Daraio C *et al* (2005). Growth of nanoscale hydroxyapatite using chemically treated titanium oxide nanotubes. *Biomaterials* **26:** 4938–4943.

Oh S, Daraio C, Chen LH *et al* (2006). Significantly accelerated osteoblast cell growth on aligned TiO_2 nanotubes. *J Biomed Mater Res A* **78:** 97–103.

Oh S, Brammer KS, Li YS *et al* (2009). Stem cell fate dictated solely by altered nanotube dimension. *Proc Natl Acad Sci U S A* **106:** 2130–2135.

Palmieri A, Pezzetti F, Brunelli G *et al* (2008). Anatase nanosurface regulates microRNAs. *J Craniofac Surg* **19:** 328–333.

Popat KC, Leary Swan EE, Mukhatyar V *et al* (2005). Influence of nanoporous alumina membranes on long-term osteoblast response. *Biomaterials* **26:** 4516–4522.

Popat KC, Leoni L, Grimes CA *et al* (2007). Influence of engineered titania nanotubular surfaces on bone cells. *Biomaterials* **28:** 3188–3197.

Qu J, Chehroudi B, Brunette DM (1996). The use of micromachined surfaces to investigate the cell behavioural factors essential to osseointegration. *Oral Dis* **2:** 102–115.

Roberts WE (1988). Bone tissue interface. *J Dent Educ* **52:** 804–809.

Sollazzo V, Palmieri A, Pezzetti F *et al* (2008). Genetic effect of anatase on osteoblast-like cells. *J Biomed Mater Res B Appl Biomater*. **85:** 29–36.

Swan EE, Popat KC, Grimes CA *et al* (2005). Fabrication and evaluation of nanoporous alumina membranes for osteoblast culture. *J Biomed Mater Res A* **72:** 288–295.

Tsuchiya H, Macak JM, Müller L *et al* (2006). Hydroxyapatite growth on anodic TiO_2 nanotubes. *J Biomed Mater Res A* **77:** 534–541.

Von Wilmowsky C, Bauer S, Lutz R *et al* (2009). In vivo evaluation of anodic TiO_2 nanotubes: an experimental study in the pig. *J Biomed Mater Res B Appl Biomater* **89:** 165–171.

Webster TJ, Ejiofor JU (2004). Increased osteoblast adhesion on nanophase metals: Ti, Ti6Al4V, and CoCrMo. *Biomaterials* **25:** 4731–4739.

Webster TJ, Siegel RW, Bizios R (1999). Osteoblast adhesion on nanophase ceramics. *Biomaterials* **20:** 1222–1227.

Webster TJ, Ergun C, Doremus RH (2000). Enhanced functions of osteoblasts on nanophase ceramics. *Biomaterials* **21**(17)**:** 1803–1810.

Yang XF, Chen Y, Yang F *et al* (2009). Enhanced initial adhesion of osteoblast-like cells on an anatase-structured titania surface formed by H_2O_2/HCl solution and heat treatment. *Dent Mater* **25:** 473–480.

Yao C, Slamovich EB, Webster TJ (2008). Enhanced osteoblast functions on anodized titanium with nanotube-like structures. *J Biomed Mater Res A* **85:** 157–166.